Investigation of *1n*-evaporation channel of Superheavy nuclei with Z=102-113

Dissertation submitted in partial fulfilment of requirement for

The award of degree of

Master of Science

In

Physics

Under

The supervision of

Dr. Manoj Kumar Sharma

(Professor)

Submitted by

Gurjit Kaur

Roll no: 301204003

School of Physics and Material Science

Thapar University

Patiala (Punjab)

147001

A SMALL CONTRIBUTION

TO

NUCLEAR PHYSICS

3

Certificate

This is to certify that Ms. Gurjit Kaur, Roll no. 301204003 has worked on this thesis report as a partial fulfilment for award degree of MASTERS OF SCIENCE in physics. I certify that the matter embodied in this report is of candidate's own record and not submitted to any other university in any part or full form for the award of such a degree.

Gurjit Kaur
7/7/14

7.7.14

Dr. Manoj Kumar Sharma
Supervisor
Professor, SPMS, Thapar University
Patiala

Countersigned by:

Dr. Kulvir Singh
(Prof. & Head)
SPMS, Thapar University
Patiala

Dr. S.K. Mahopatra
Dean Of Academic Affairs
Thapar University
Patiala

4

Acknowledgement

My vocabulary runs short to find the appropriate words to express the deep gratitude and respect to my guide Dr. Manoj Kumar Sharma, Professor, School of Physics and Material Science, Thapar University, Patiala for his myriad suggestion, fruitful guidance and strong motivation during the completion of my thesis work. I express my sincere thanks to him for providing me the vast knowledge about Nuclear Physics and his cooperation and encouragement, without which I would never succeeded in completing my task. I am sure, the knowledge that I achieved through association with my supervisor shall stay long to realize and achieve the ultimate aim of my carrier.

I also thanks Dr. Kulvir Singh, Prof. and Head, school of Physics and Material Science for his support and providing facilities.

A few special words of thanks from bottom of my heart to Ms. Kirandeep Sandhu, Research Scholar for her timely help, valuable suggestion whenever I needed out of her busy schedule. Her support and keen interest helped me to do better in my thesis work.

I am deeply thankful to my family, without whom I am nothing for their moral support, great opportunities, encouragement and lots of love. I am also thankful to all my friends for providing me friendly atmosphere and encouraging me throughout the work.

Gurjit Kaur

Date: 7 July, 2014 (Ms. Gurjit Kaur)

Abstract

Synthesis of superheavy nuclei (SHN) is a long-standing important subject of nuclear physics. The new elements which are synthesised are extremely important because they are expected to have new properties which may address some unresolved issues related to nuclear dynamics. Now a day the synthesis of SHN is getting more and more challenging due to smaller production cross-section either for cold or for hot fusion-evaporation reactions. Thus the appropriate theoretical research of existing methods is needed for proper understanding of dynamical aspect of superheavy nuclei.

Keeping this in mind, we studied the *1n*-decay pattern of a number of heavy/superheavy nuclei using hot and cold optimum orientations within dynamical cluster decay model (DCM) by considering β_2 – deformations. In the present work we discuss *1n* decay channel using Pb and Bi targets for nuclei lying in the range Z=102-113 within energy range E_{CN}^{*}=10.61-28.9 MeV. In the decay of these nuclei various factors such as fragmentation potential (V), preformation probability (P_0) and penetrability (P) are analysed by fitting the neck length parameter ΔR of the model. In addition to this we have also investigated the exclusive role of deformations for these nuclei. Finally the comparative analysis of sticking and non-sticking moment of inertia is carried out by inspecting respective fragmentation paths.

CONTENTS

List of Figures and Tables

Chapter-1

Chapter-2

Chapter-3

List of Table:-

CHAPTER-1

INTRODUCTION

Inception of Nuclear physics started about a century ago during the "miraculous decade" between 1895 and 1905 when the foundation of modern physics was being completely established. Parallel to the unexpected results of the Crooke's vacuum tube: Roentgen's X-rays (1895) and Thomson's electron (1897), the major impact to this concept was contributed by the phenomenon of radioactivity, introduced in 1896 by Henry Becquerel [1]. For the first time it was observed that the nucleus of an atom disintegrates itself by emitting α, β and γ-rays. With this concept, the new frontiers of the physical world were opened and enormous experimental and theoretical research was then carried out to understand the behaviour of nucleus and its properties.

After this, the journey of the nuclear science had turned its path towards the search of the new elements in which the radioactive elements were used as the probe to reach the land of heavy and superheavy elements. The creation of elements with atomic number beyond that of Uranium is challenging, as the half-life of elements decreases with increasing atomic number. Fig.1.1 shows the experimental developments to climb up the periodic table element by element by understanding the different periods of nuclear science.

1.1 Experimental developments:-

Fig.1.1depicts the primordial elements U and Th, and shows the next period (1934–1955) in which the manmade (artificial) elements from Z=93 to Z=100 were synthesised via neutron and α-capture reactions. These processes were considered as the primitive step for the production the heavy nuclei. For example, Plutonium-239 is synthesized via the neutron capture reaction using uranium (U) and neutrons (n) via beta decay (β^-) with Neptunium (Np) as an intermediate nucleus.

$$^{238}_{92}U + {}^{1}_{0}n \longrightarrow {}^{239}_{92}U \xrightarrow{\beta^-} {}^{239}_{93}Np \xrightarrow{\beta^-} {}^{239}_{94}Pu$$

Due to high Coulomb forces, further in 1955–1974 heavier actinides and other elements were produced in nuclear reactors by fusing isotopes of the light nuclei B to O with actinide targets (Z<100) [2]. Using this, the last produced element was Z=106. Finally from 1974 to till date, the various elements ranging from Z=107 to Z=118 were synthesised in hot and cold fusion reactions which are described later in Sec.1.3. The high experimental facilities in the last

period of nuclear physics had provided the great opportunity to nuclear world to reach the island of stability proposed for the superheavy elements.

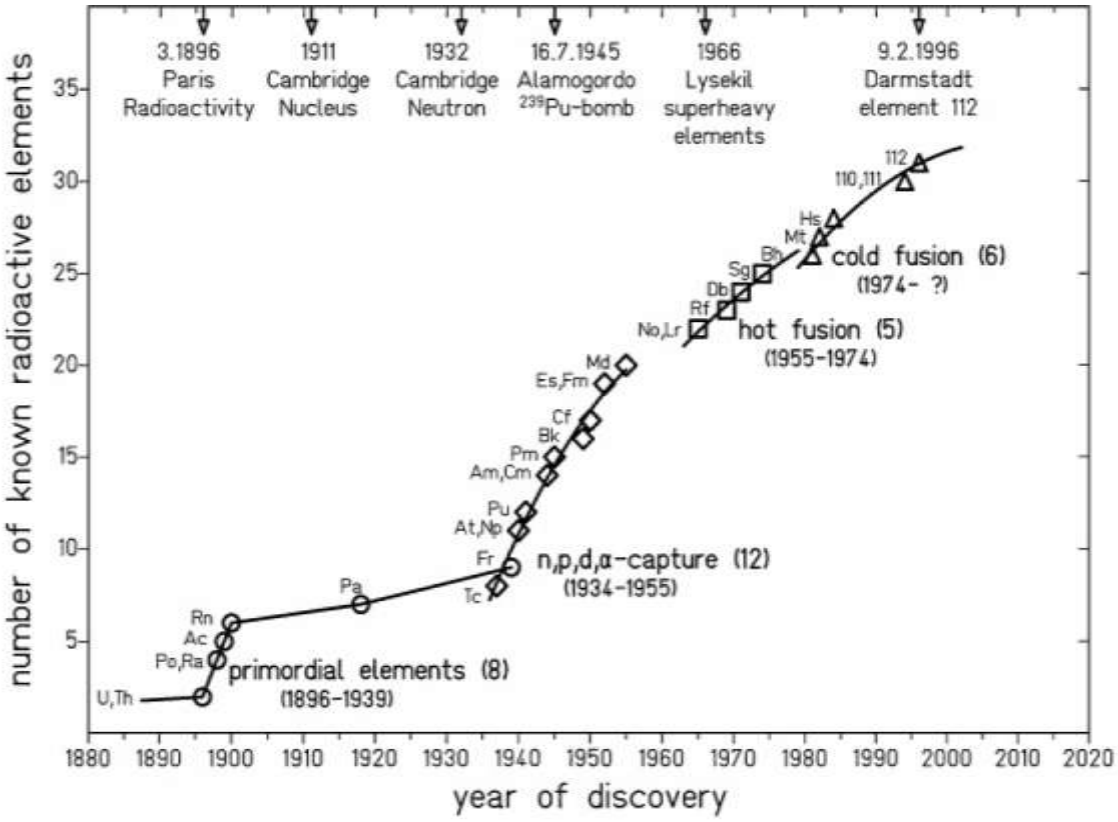

Fig.1.1 Chart of radioactive elements representing the different periods of nuclear physics [2].

1.2 Theoretical developments:-

The formation and decaying scenario of the heavy and superheavy nuclei is relatively complex. According to macroscopic point of view, their production could not be possible with the atomic number beyond Z ~100 [3]. According to Bohr and Wheeler, the nuclear matter is considered as charged liquid drop in which the nuclear force balances the force of electric (Coulomb) repulsion of protons. On the other hand the situation changes drastically with increasing number of protons and neutrons. As soon as the drop reaches some critical deformation in the process of counter action of these two forces, it divides into two parts i.e. fission takes place. Hence, as we approach the higher elements with Z>100, the Coulomb forces start competing the binding energy of the nucleus [3].

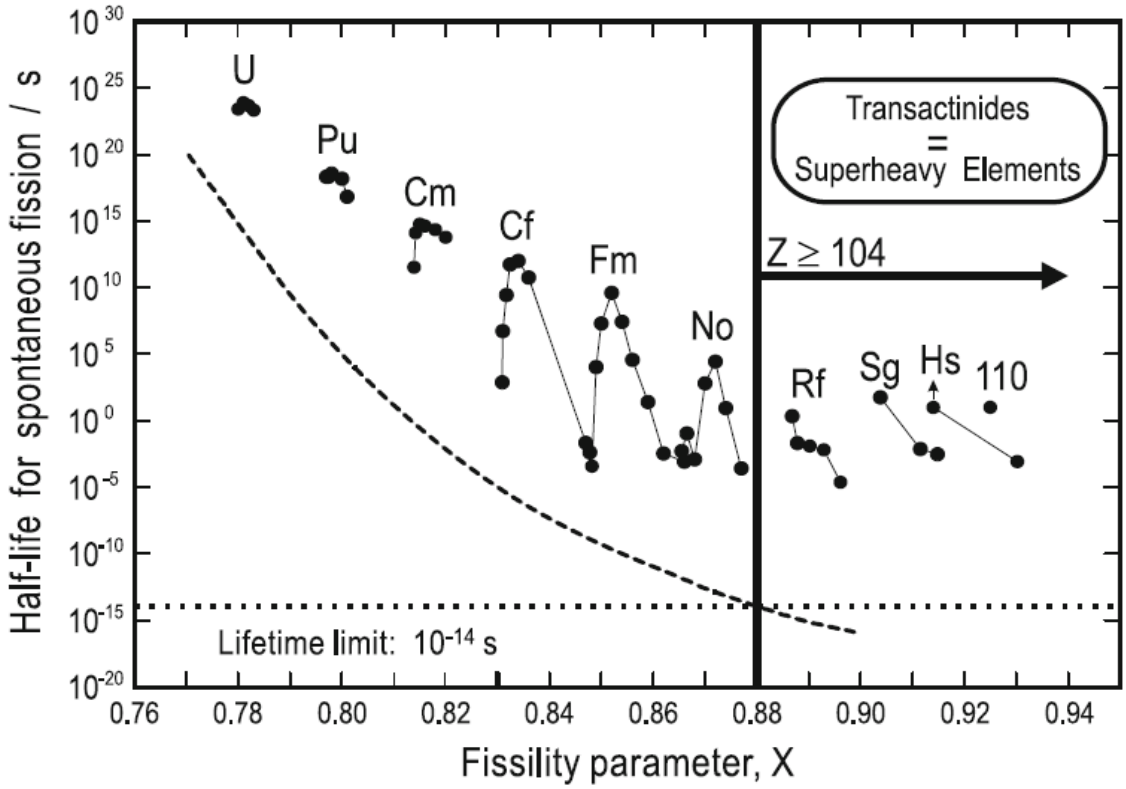

Fig 1.2. Experimental spontaneous fission half-lives for even-even nuclei (circles) compared to the prediction of the liquid drop model as a function of the fissility parameter $X= Z^2/A$ (dashed line) [4].

The stability of nucleus against fission in LDM can be described by fissility parameter which is approximately given by $X=Z^2 / A$. Fig. 1.2 shows the experimentally obtained spontaneous fission half-lives for number of heavy/superheavy nuclei and compared with the fission half-lives predicted by the LDM alone. The horizontal dotted line shows the minimum lifetime for the formation of a chemical element. From the above figure, we can clearly see that the spontaneous fission half –lives calculated for Rf (Z=104), Sg (Z=106) and Hs (Z=108) drop below the minimum lifetime for formation of nucleus. Hence under such condition the further penetration to the land of extreme mass looks quite difficult. The reasonable remedy to this problem is provided by the introduction of the shell model [5-6] (shown in Fig. 1.3) based upon spin orbit interaction. According to this model, for higher elements, the necessary balance between Coulomb forces and nuclear forces is achieved by shell stabilisation effects [7-8]. For example, the prediction of proton or neutron magic at Z or N=126 is due to the splitting of $1i$ into $1i_{13/2}$ and $1i_{11/2}$,where i correspond to orbital angular momentum ℓ=6.

From Fig.1.3 it is clear that due to spin orbit interaction, the 14 nucleons of $1i_{13/2}$ were pushed downward to complete the magicity around Z or N=126.

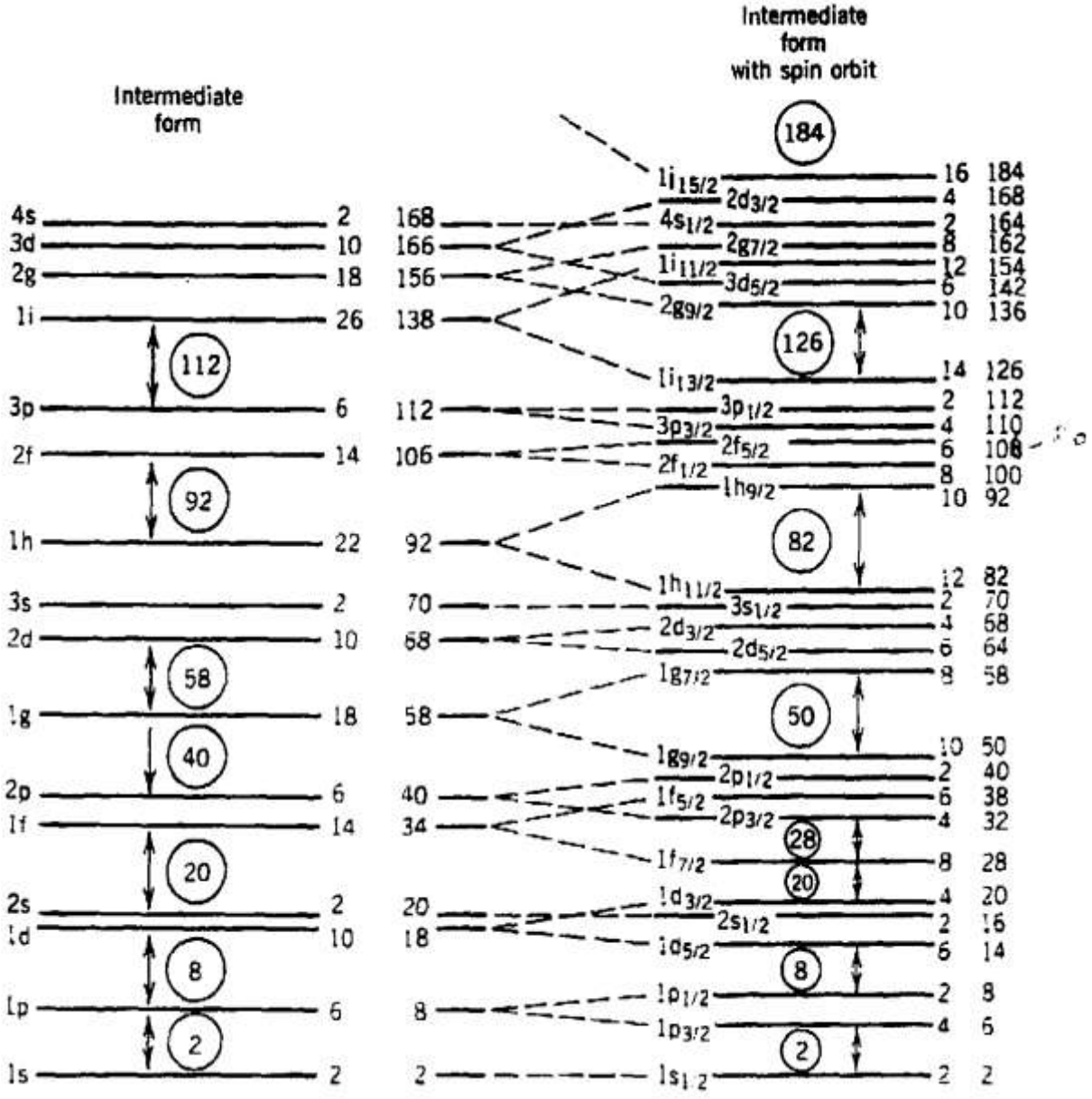

Fig. 1.3 Schematic representation of states and magic numbers in shell model [9].

On the other hand, the magic shell closure with Z=114 is realised if a large spin-orbit splitting takes place between $2f_{5/2}$ and $2f_{7/2,}$ however Z=120 appears if small spin-orbit force starts acting between the same orbital, as shown in Fig 1.4. Hence Z=126, 120 and 114 can be considered as the possible magic candidates to locate the island of stability for the superheavy mass region.

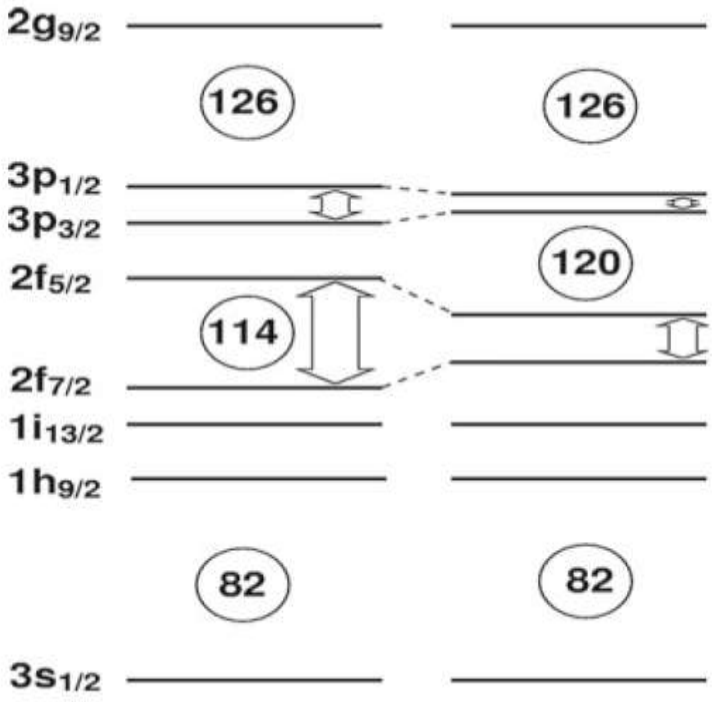

Fig. 1.4 Shell model representing the proton gaps at Z=114 and 120 in addition to Z=126 [4].

Based upon shell model, various theories were developed to resolve the issue of different magicity. The first theory was the macro-microscopic formalism [10-11] in which liquid drop and shell corrections both are included. Some models based upon the MM theory predicted the magic shell closure at Z=114 and N=184. On the other hand, some relativistic and non-relativistic self-consistent microscopic models also proposed the stability around Z=120 and Z=126 with N=184 [12-15]. Hence it is clear from the above discussion that the identification of proton magic shell closures is an ongoing quest for the superheavy mass region. On the other hand, the neutron magicity at N=184 is the consequence of most of the theoretical studies. In addition to this, some relativistic mean field models also suggested the neutron magic stability around N=172 [16].

To attain the proposed magicity for superheavy nuclei, numerous experimental studies were made through heavy ion reactions with the use of spherical as well as deformed (prolate) targets via cold and hot fusion process respectively, in different laboratories such as GSI, RIKEN, JINR, and DUBNA.

1.3 Synthesis of SHE:-

The superheavy elements are produced in heavy- ion reactions by complete fusion involving the amalgamation of two heavy species. It has been commonly accepted that fusion of heavy nuclear systems is hindered as compared to that of light nuclear systems. Consequently, the formation of superheavy nuclei is severely hindered and the cross sections for the synthesis of heaviest elements are extremely small. Therefore it is very important to select the optimal projectile-target combination for the successful synthesis of superheavy nuclei. On the basis of this, two different fusion reactions were proposed for the formation of superheavy elements such as hot and cold fusion reactions.

1.3.1 Hot Fusion:-

In this method of fusion, usually the actinide targets are collided with light projectiles varying from Boron to Oxygen. This kind of interaction generates the hot compound nucleus (CN) in the excitation energy range of 30-50 MeV. By using this method, elements from Z=101-106 were synthesised with the emission of 3-5 neutrons from the compound nucleus.

For example, by the emission of 5 neutrons form the ^{266}Rf * compound nucleus formed in ^{18}O + ^{248}Cm, the stable isotope of Z=104 is produced [17].

$$^{18}O + {}^{248}Cm \rightarrow {}^{266}Rf^{*} \rightarrow {}^{261}Rf + 5n$$

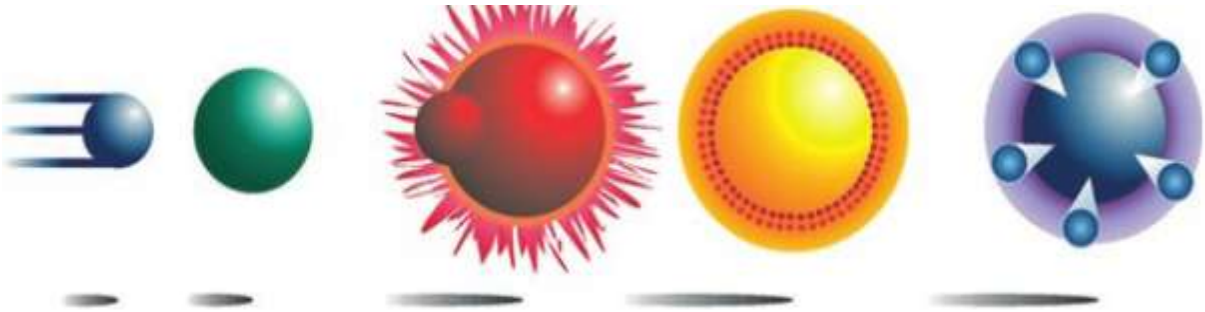

*Fig 1.5. Hot fusion reaction of ^{18}O +^{248}Cm to form ^{266}Rf * compound nucleus.*

Limitation of hot fusion reaction:-

With increasing the projectile-target mass, the excitation energy of compound nucleus increases due to increase in Coulomb energy. This result in:-

(1) Decrease in survival probability of evaporation product at fast rate with increasing excitation energy [18].

(2) Suppression in the shell effects in the nuclei with increase in excitation energy of the compound nucleus [18].

Both these factors lead to extremely small survival probability of heavy compound nucleus and limit the elements up to 106.

Due to small production probability with increasing atomic number, modification was required to produce higher superheavy elements. For this, instead of light projectiles used in hot fusion process, doubly magic ^{48}Ca [19] was suggested to move towards the island of stability. In this process the compound nuclei with excitation energy 10 MeV less were produced than the traditional range of the hot fusion interaction. Using this method, elements from 113-118 was produced [19]-[20] and was later tested for lighter superheavy nuclei also. This method is relatively useful due to following reasons:-

(1) At this excitation energy shell effect is still noticeable and probability of survival of evaporation product is larger than the earlier process.

(2) At the same time the mass asymmetry in entrance channel reduces the suppression of fusion and hence the cross section for CN formation increases.

(3) Superheavy nuclei are formed with the neutron excess lying closer to the N=184 neutron magic.

1.3.2 Cold fusion reactions:-

The next production process proposed for the formation of superheavy elements were the cold fusion reaction in which usually spherical target material is used. Within this process the compound nucleus with high survival probability is produced because the disintegration of CN generally takes place via evaporation of 1 or 2 neutrons and gamma rays at low excitation energies in the range of 10-20 MeV. With this method, the elements from Z=107 to 112 were successfully synthesised by using ^{208}Pb and ^{209}Bi targets.

Some reactions representing cold fusion process of SHN are as given below:-

(1) $^{208}Pb + {}^{51}V \rightarrow {}^{258}Db + 1n$ [21]

(2) $^{209}Bi + {}^{58}Fe \rightarrow {}^{266}Mt + 1n$ [22]

The example of cold fusion reaction is shown below in which ^{265}Hs nucleus is formed after evaporating 1 neutron [23].

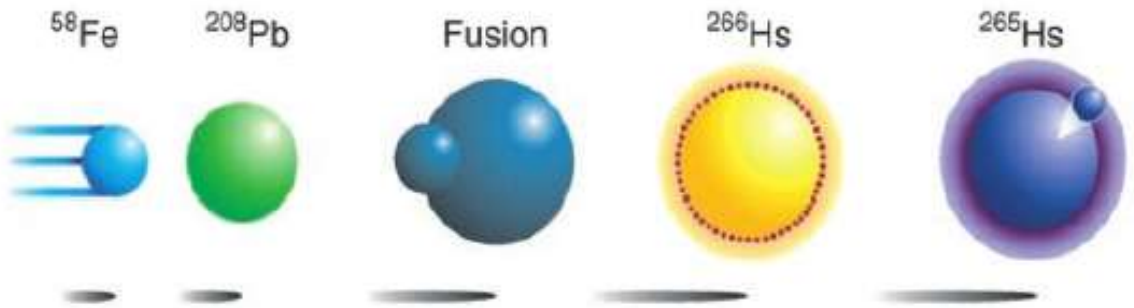

Fig 1.6 Cold Fusion reaction of $^{58}Fe+^{208}Pb$ to form $^{266}Hs^*$ compound nucleus.

But further to achieve higher atomic number with cold fusion process is not possible due to following reasons:-

(1) Due to increase in the mass of projectile, the mass asymmetry between projectile and target decreases which results in fusion hindrance [24].

(2) The nucleus produced via cold fusion reaction contains less number of neutrons [24].

For example in Z=112 we have only 165 neutrons, which are reasonably less than the predicted neutron number for superheavy nuclei.

Due to these reasons the production of elements is limited up to Z=112.

As superheavy elements formed via hot and cold fusion processes are extremely unstable , so they disintegrate by following various decay modes which are discussed as follows:-

1.4 Decay modes of superheavy Nuclei:-

Superheavy nuclei are unstable due to substantial amount of protons; hence they follow various decay mechanisms in the excited as well as in ground state. In excited state, the superheavy nuclei formed via cold and hot fusion processes usually follow the path of neutron evaporation as well as the fusion-fission. However the possibility of non-compound nucleus decay such as deep-inelastic collision and quasi-fission is also sustained. The excited state decay modes of compound nucleus are shown in Fig 1.7.

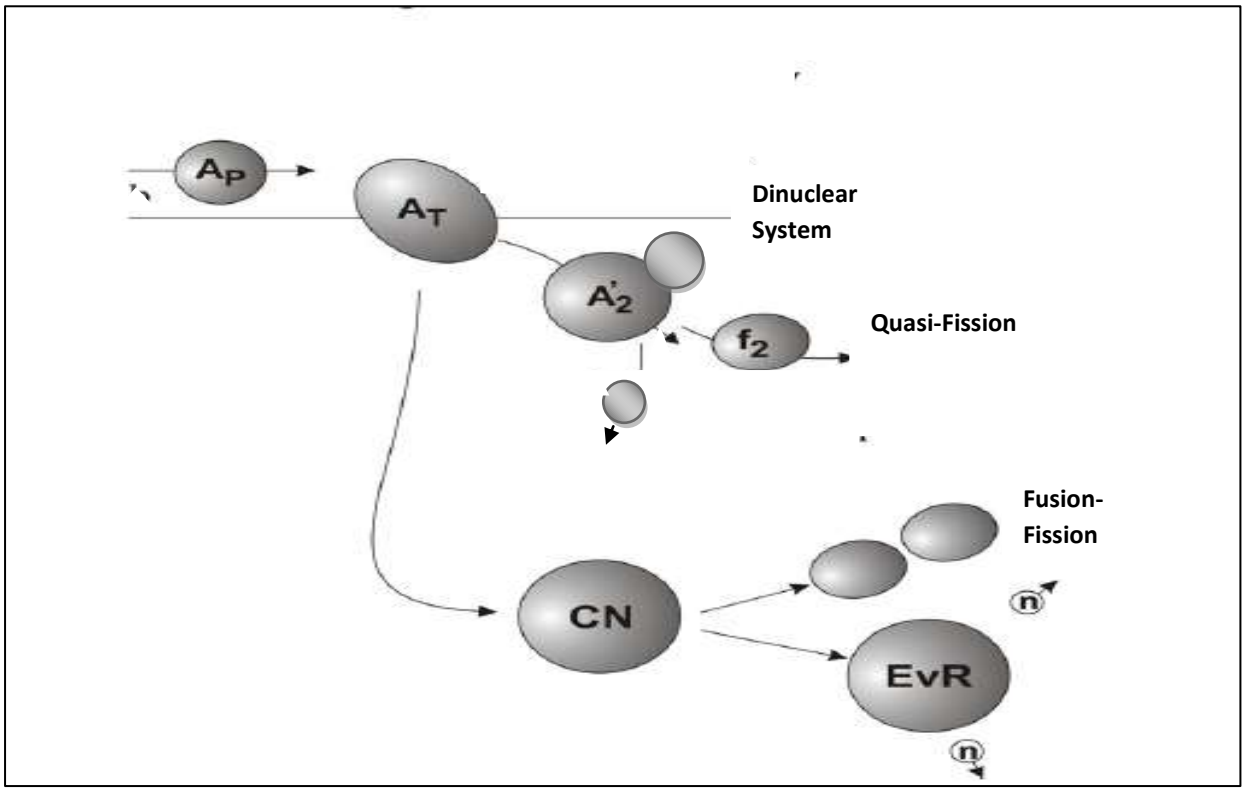

Fig1.7. Excited state decay modes of the superheavy nuclei

Broadly speaking if the projectile and the target during collision overcome the Coulomb repulsion and reach an attractive potential pocket due to strong nuclear forces then a fused dinuclear system may form a composite system known as compound nucleus [25]. This composite-system may de-excite through light-particle evaporation and fission. The light particles which may be emitted during evaporation residue formation are proton, neutron, gamma rays or α-particles, but neutron emission is more common in superheavy region. On the other hand, if the di-nuclear system is not equilibrated in all degrees of freedom, the chances for the production of non-compound nuclear system cannot be denied which may disintegrates before reaching the fission saddle point. Such non-compound nuclear decays are categorised as: quasi-fission and deep inelastic collision. The compound and non-compound nucleus phenomenon, particularly fusion-fission and quasi-fission, may be distinguished on the basis of the fragment mass distribution. Usually for fusion-fission process, mass symmetric events are involved where for quasi-fission, the asymmetric fragments contribute the most [25-26].

In addition to the excited state decays, the superheavy nuclei, also disintegrates via ground state α-decay and spontaneous fission due to small half-lives for such channel. Alpha emission is a Coulomb repulsion effect. It becomes increasingly important for heavy nuclei because the Coulomb forces increases with size at a faster rate than nuclear binding forces. For superheavy nuclei, α-decay is possible only if the shell effect supply extra binding energy to have high fission barriers. In course of α-decay chains, the shell effects gradually become weaker and finally the chain is terminated via spontaneous fission [27].

In reference to the above literature of superheavy elements, the attempt is made through the dynamical cluster decay model [28-31] to understand the reaction dynamics of various superheavy nuclei formed in the 1*n* evaporation channel by employing the dynamical cluster decay model (DCM). The role of deformations within 'hot' and 'cold' optimum orientations is analysed within this approach. Finally the effect of angular momentum is also explored by addressing the decay of superheavy nuclei through sticking and non-sticking moment of inertia. The nuclei with Z=102-113 are investigated to have comprehensive idea about 1n-evaporation process observed in heavy/superheavy nuclei.

References:-

[1] H. Becquerel, Compt. Rend. **122**, 420 (1896).

[2] P. Armbruster, Annu. Rev. Nucl. Part. Sci. **50,** 411 (2000).

[3] N. Bohr, J. A. Wheeller. Phys. Rev. **56**, 426 (1939).

[4] Rolf-Dietmar Herzberg, M. Schädel and D. Shaughnessy (eds.), "The Chemistry of Superheavy Elements "(2014).

[5] O. Haxel , J.H.D Jensen and H.E. Suess, Phys. Rev. **75,** 1766 (1949)

[6] M. G. Mayer, Phys. Rev. **75,** 1969 (1949).

[7] S. G Nilsson, C.F Tsang, A. Sobiczewski ,Z. Szyma´nski , S. Wycech , C. Gustafson , I.L Lamm, P. Moller P and B. Nilsson, Nucl. Phys. A **131,** 1 (1969).

[8] B. R Mottelson and S .G Nilsson, Phys. Rev. **99,** 1615 (1955).

[9] M. G. Mayer and J. H. D. Jensen, "elementary theory of Nuclear shell", New York, 1955.

[10] U. Mosel and W. Greiner, Z. Phys. **222**, 261 (1969).

[11] S. G. Nilsson, C. F. Tsang, A. Sobiczewski, Z. Szymanski, S. Wycech, C. Gustafson, I.-L. Lamm, P. Moller, and B. Nilsson, Nucl. Phys. A **131**, 1 (1969).

[12] K. Rutz, M. Bender, T. Burvenich, T. Schilling et.al. Phys. Rev. C **56**, 238 (1997); M. Bender, K. Rutz. P. G. Reinhard, J. A. Maruhn, and W. Greiner, ibid **60**, 034304 (1999).

[13] R. K. Gupta, S. K. Patra and W. Greiner, Mod.Phys. let. A **12**, 1727(1997); S.K. Patra, C.L. Wu, C. R. Preharaj and R. K. Gupta, Nucl. Phys. A **651**, 117 (1999).

[14] W. Myers and W. J. Swiatecki, Nucl. Phys. **81**, 1 (1966).

[15] A.T. Kruppa, M. Bender, W. Nazarewicz, P.G. Reinhard T. Vertse and S. Cwiok, Phys. Rev. C **61**, 034313 (2000).

[16] M. Bhuyan, S. K. Patra, and R. K. Gupta, Phys. Rev. C **84**, (2011).

[17] Y. Nagame, M. Asai, H. Haba, S. Goto, K. Tsukada, I. Nishinaka, K. Nishio, S. Ichikawa, A. Toyoshima, K. Akiyama, H. Nakahara, M. Sakama, M. Schnabel, Journal of Nuclear and Radiochemical Sciences **3**, 85 (2002).

[18]Yu. Ts. Oganessian, Pure Appl. Chem., **76**, 1715 (2004).

[19] Yu. Ts. Oganessian, Phys. Rev. Lett. **109**, 162501 (2012).

[20] Yu. Ts. Oganessian**,** J. Phys. G: Nucl. Part. Phys. **34** 165–242 (2007).

[21] J. M. Gates et al., Phys. Rev. C **78**, 034604 (2008).

[22] S. Hofmann, Rep. Prog. Phys. **61**, 639 (1998),

[23] S. Hofmann et al., Nucl. Phys. A **734**, 93 (2004).

[24] Yu. Ts. Oganessian, Pure Appl. Chem., **78**, 889 (2006).

[25] T. K. Ghosh, Nucl. Phys. **56** (2011).

[26] R. K. Choudhury and R. G. Thomas, Journal of Physics **282**, 012004 (2011).

[27] I. Silisteanu, M. Rizea, B. I. Ciobanu, A. Neacsu, Rom. Journ. Phys. **53,** 1191-1197 (2008).

[28] B. B. Singh, M. K. Sharma, R. K. Gupta and W. Greiner, Int. J. Mod. Phys. E15, 699 (2006) ; B. B. Singh, M. K. Sharma, R. K. Gupta, Phys. Rev. C 77, 054613 (2008).

[29] Niyti, R. K. Gupta, and W. Greiner, J. Phys. G **37**, 115103 (2010).

[30] R. K. Gupta and M. Bansal, Int. Rev. Phys. (I.RE.PHY.) **5**, 74 (2011).

[31] M. K. Sharma, G. Sawhney, R. K. Gupta, and W. Greiner, J. Phys. G **38**, 105101 (2011); M. K. Sharma, G. Sawhney, R. K. Gupta, W.Greiner, J. Phys. G: Nucl. Part. Phys. **38** 105101 (2011).

CHAPTER-2

The Dynamical Cluster Decay Model (DCM)

The formation and decay of massive nuclei have been a topic of great interest. The understanding of the properties of the nucleus via macro-microscopic [1-3] analysis, relativistic and non-relativistic [4-7] approaches show the importance of theoretical studies for the superheavy mass region. The model used in the present work for the study of synthesis of superheavy elements is DCM [8-15] based on Quantum Mechanical Fragmentation theory (QMFT) [16-19] where potential is calculated by macroscopic-microscopic method.

Dynamical cluster decay model (DCM) is used to study the decay of hot and rotating compound nuclei using collective clusterization technique for the emission of ER, IMF, HMF as well as fission. Interesting aspect about DCM is that, contrary to statistical approach it treats different decay possibilities on equal footing.

2.1 Introduction to DCM:-

The Dynamical Cluster Decay Model (DCM) [8-15] is a reformulation of the Preformed Cluster Model (PCM) [20-22] for ground-state decays such as cluster radioactivity (CR), spontaneous fission and related phenomena. DCM and PCM works alike, the only difference is DCM is used in reference to study the decay of hot and rotating nuclei (i.e. angular momentum and temperature both are included) and Preformed Cluster Model is used to study the ground state decay at $\ell = 0$ and t=0.

DCM (dynamical cluster decay model) has been established for the study of heavy ion reaction dynamics especially for the decay of excited compound nucleus. The deformations and orientations effects of reaction partners and decay products are explicitly included in this model along with temperature and angular momentum contributions. This model is worked out in terms of only one parameter fitting, the neck-length parameter ΔR because the fission path is obtained by minimization of potential surface with respect to neck length parameter (ΔR) and mass and charge asymmetry. According to definition ΔR is relative separation distance between two fragments.

DCM worked out in two terms that are

(a) mass asymmetry $\eta = \frac{A2-A1}{A2+A1}$, which gives the nucleon-division (or -exchange) between outgoing fragments and

(b) relative separation R which give transfer of kinetic energy of incident channel ($E_{c.m.}$) to internal excitation (total excitation or total kinetic energy, TXE or TKE) of the outgoing channel.

Temperature dependent excitation energy is given by

$$E^*_{CN} = (A/11)\, T^2 - T \qquad (2.1)$$

Since the fixed R = Ra (defined later), at which the process is calculated, depends on temperature T as well as on η, i.e. R (T, η). This energy transfer process is given by relation

$$E^*_{CN} = E_{c.m.} + Q_{in} \qquad (2.2)$$

This model is a two-step model:-

(a) First step is quantum mechanical preformation probability P_0 of the decay products or cluster formed in the mother nucleus.

(b) Second step is the penetration of the fragments/ clusters through the interaction barrier.

These two quantities are used to calculate the cross-sections which is given as:-

$$\sigma = \frac{\pi}{k^2}\sum_{l=0}^{\ell_{max}}(2l+1)P_0P \quad , \quad k = \sqrt{\frac{2\mu E_{c.m}}{\hbar^2}} \qquad (2.3)$$

where, P_0, the preformation probability and P, the penetrability. Preformation probability refers to the motion in mass asymmetry coordinate $\eta = \frac{A_1 - A_2}{A_1 + A_2}$; (1 and 2 represent heavy and light fragments) and the penetrability P to relative separation R motion. Both preformation probability and the penetrability depend on ℓ and T of the system, and on deformations $\beta_{\lambda i}$ and orientations θ_i of the two nuclei or fragments. (λ=2, 3, 4, for quadrupole, octupole, hexadecapole deformations)

2.2 Preformation probability P_0:-

The structure information of the CN enters the model via preformation probability P_o (also known as spectroscopic factor) of the fragments given by the solution of stationary Schrodinger equation in η which is given below:

$$H = \frac{-\hbar^2}{2\sqrt{B_{\eta\eta}}}\frac{\partial}{\partial\eta}\frac{1}{\sqrt{B_{\eta\eta}}}\frac{\partial}{\partial\eta} - \frac{\hbar^2}{2\sqrt{B_{RR}}}\frac{\partial}{\partial R}\frac{1}{\sqrt{B_{RR}}}\frac{\partial}{\partial R} + V(\eta) + V(R) \quad (2.4)$$

Schrodinger wave equation can be separated for the two co-ordinates η and R as follows,

$$\left[\frac{-\hbar^2}{2\sqrt{B_{\eta\eta}}}\frac{\partial}{\partial\eta}\frac{1}{\sqrt{B_{\eta\eta}}}\frac{\partial}{\partial\eta} + V(\eta)\right]\Psi^v(\eta) = E_\eta^v\Psi^v(\eta) \quad (2.5)$$

$$\left[\frac{-\hbar^2}{2\sqrt{B_{RR}}}\frac{\partial}{\partial R}\frac{1}{\sqrt{B_{RR}}}\frac{\partial}{\partial R} + V(R)\right]\Psi^v(R) = E_R^v\Psi^v(R) \quad (2.6)$$

With ψ (η, R) = ψ (η) ψ(R)

$E = E_\eta + E_R$

The states Ψ^vs (η) are the vibrational states in the potential V (η) and are labelled by the quantum numbers $\boldsymbol{v}$ =0, 1, 2……$B_{\eta\eta}(\eta)$ is smooth classical hydro dynamical masses and represents the kinetic energy part in Eq.(2.5).

The solutions of Eq. (2.5) give the preformation probability at a fixed $R=R_a$ as following:-

$$P_0 \propto |\psi^0(\eta)|^2$$

$$or \quad P_0 = \sqrt{B_{\eta\eta}}\,|\,\Psi[\eta(A_i)]\,|^2\,(\tfrac{2}{A}) \quad (2.7)$$

The potential used in this Schrodinger equation is given by:

$$V(R,\eta,T) = [V_{LDM}(Ai, Zi, T) + \sum_{i=1}^{2} [\delta Ui]\exp(-T^2/T_o^2) + Vc(Zi, \beta_{\lambda i}, \theta i, T) + V_P(A, \beta_{\lambda i}, \theta i, T)$$

$$+ V_l(R, \beta_{\lambda i}, \theta i, T). \quad (2.8)$$

where the T-dependent terms V_c, V_P and V_l are defined as follows: V_c is the Coulomb potential, V_P is the proximity potential for hot deformed nuclei and V_l is the potential due to rotational motion of hot deformed nuclei.

Further, in Eq. (2.8), within the Strutinsky renormalization procedure, one can define the binding energy B of a nucleus at temperature T as the sum of liquid drop energy V_{LDM} (T) and shell correction δU (T) i.e.

$$B(T)=V_{LDM}(T)+\delta U\exp(\frac{-T^2}{T_0^2}) \quad (2.9)$$

The T dependent liquid drop part of binding energy $V_{LDM}(T)$ is calculated from Davidson et.al.[23] based on the semi-empirical mass formula of Seeger [24]. For the second part of equation which represent the shell correction we use the empirical formula of Myers and Swiatecki[25].

2.3 Potential Used In Schrodinger Equation:-

The remaining three terms in equation(2.8) can be explained as follows:-

2.3.1 Coulomb Potential (V_C):-

Coulomb potential describes the force of repulsion between two interacting nuclei due to their charges. It acts along the line joining the two nuclei. For interacting deformed and oriented nuclei, different authors [26]-[27] have derived it differently.

The Coulomb potential for hot and rotating, deformed and oriented nuclei given as:

$$V_c(Z_i,\beta_{\lambda i},\theta_i,T) = \frac{Z_1Z_2e^2}{R(T)} + 3Z_1Z_2e^2\sum_{\lambda,i=1,2}\frac{R_i^{\lambda}(d_i,T)}{(2\lambda+1)R(T)^{\lambda+1}} \quad (2.10)$$

2.3.2 The Proximity Potential for deformed, oriented and coplanar nuclei (V_P):-

When two surfaces approach each other within a small distance of less than ~ 2fm, comparable with the surface thickness of interacting nuclei is when two surfaces start facing each other across a small gap, then the surface energy term alone could not give rise to the strong attraction that is observed when the two surfaces are brought in close proximity. Such additional attractive forces are called proximity forces and the additional potential due to these forces is called the nuclear proximity potential.

Blocki et.ai. [28] have reanalysed and extended a theorem, originally formed by Deryagin [29] according to which the force between two gently curved surfaces in close proximity is proportional to the interaction potential per unit area between the two flat surfaces. The original expression of Blocki based on the pocket formula was for spherical nuclei, and is and give the expression:-

$$V_P(s_0) = 4\pi\overline{R}\gamma b\Phi(s_0). \quad (2.11)$$

$\Phi(s_0)$ is the universal function, independent of the shapes of nuclei or the geometry of nuclear system,but depends on the minimum separation distance(s_0), b is the diffuseness of the nuclear surface and γ is the specific nuclear surface tension given by:

2.3.3 Rotational Energy Due To Angular Momentum:-

The rotational motion gives an additional energy due to the angular momentum defined as:-

$$V_l(T) = \frac{\hbar^2 l(l+1)}{2\mu R^2} \quad (2.12)$$

With $I=\mu R^2$, is the non-sticking moment of inertia with μ as reduce mass. In complete sticking limits, the moment of inertia I is given by:

$$I=\mu R^2 + \frac{2}{5} A_1 m R_1^2 + + \frac{2}{5} A_2 m R_2^2 \quad (2.13)$$

It is relevant to mention here that value of angular momentum extracted experimentally, is based on moment of inertia limit. In present work a comparative analysis of sticking and non-sticking moment of inertia is worked out to address 1n evaporation channel of a variety of superheavy nuclei within even and odd Z-values.

2.4 PENETRABILITY (P):-

Penetrability (P) is calculated as the WKB tunnelling probability solved analytically and is given by:

$$P = \exp[-\frac{2}{\hbar}\int_{R_a}^{R_b}\{2\mu[V(R)-Q_{eff}]\}^{1/2} dR] \quad (2.14)$$

Here $R_a = R_1(\alpha_1,T) + R_2(\alpha_2, T) + \Delta R(T)$ or $R_a = R_t + \Delta R(T)$ (2.15)

The constant $R = R_a$ (as shown in Fig.2.1) fixed empirically as the first turning point of the penetration path for the ground state (g.s, T=0) decay, this value of R (instead of CN radius R0) assimilates the effects of the deformations of two fragments and neck formation between them.

The radius vector $R_i(\alpha,T)$ is given by :

$$R_i(\alpha_i, T) = R_{0i}(T)\left[1+\sum_{\lambda}\beta_{\lambda i}Y_{\lambda}^{(0)}(\alpha_i)\right] \quad (2.16)$$

Where $R_{0i}(T)$ is given below:

$$R_{0i}= [\ 1.28A_i^{1/3}-0.76+0.8A_i^{-1/3}\ ]\ (\ 1+0.0007T^2\ ) \quad (2.17)$$

The potential corresponding to R_a i.e $V(R_a)$ act like effective Q value for decay of hot CN at particular temperature and is defined as:

$$V(R_a,T)=Q_{eff}(T)=B_{CN}(T) - [\ B_P(T=0) + B_T(T=0)\ ] \quad (2.18)$$

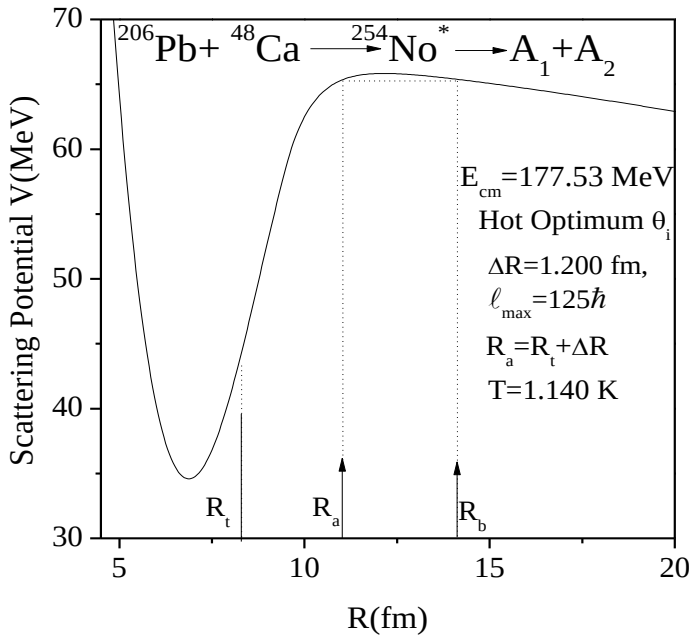

Fig.2.1. Scattering potential Plot for 1n decay of ^{254}No formed in ^{206}Pb+^{48}Ca ⟶ ^{254}No* reaction*

References:-

[1] U. Mosel and W. Greiner, Z. Phys. **222**, 261 (1969).

[2] S. G. Nilsson, C. F. Tsang, A. Sobiczewski, Z. Szymanski, S. Wycech, C. Gustafson, I.-L. Lamm, P. Moller, and B. Nilsson, Nucl. Phys. A **131**, 1 (1969).

[3] Z. Patyk and A. Sobiczewski, Nucl. Phys. A **533**, 132 (1991).

[4] W. Myers and W.J. Swiatecki, Nucl. Phys. **81**, 1 (1966).

[5] K. Rutz, M. Bender, T. Burvenich, T. Schilling et.al. Phys. Rev. C 56, 238 (1997); M. Bender, K. Rutz. P. G. Reinhard, J.A. Maruhn, and W. Greiner, ibid **60**, 034304 (1999).

[6] R. K. Gupta, S. K. Patra and W. Greiner, Mod. Phys. lett. A **12**, 1727(1997); S. K. Patra, C.L. Wu, C. R. Preharaj and R.K. Gupta, Nucl. Phys. A **651**, 117 (1999).

[7] A. T. Kruppa, M. Bender, W.nazarewicz, P. G. Reinhard T. Vertse and S. Cwiok, Phys. Rev. C **61**, 034313 (2000).

[8] B. B. Singh, M. K. Sharma, R. K. Gupta and W. Greiner, Int. J. Mod. Phys. E15, 699 (2006) ; B. B. Singh, M. K. Sharma, R. K. Gupta, Phys. Rev. C 77, 054613 (2008).

[9] Niyti, R. K. Gupta, and W. Greiner, J. Phys. G **37**, 115103 (2010).

[10] R. K. Gupta, S. K. Arun, R. Kumar and Niyti Int. Rev. Phys. (IREPHY) **2**, 369 (2008); R. K. Gupta and M. Bansal, Int. Rev. Phys. (I.RE.PHY.) **5**, 74 (2011).

[11] M. K. Sharma, G. Sawhney, R. K. Gupta, and W. Greiner, J. Phys. G **38**, 105101 (2011); M. K. Sharma, G. Sawhney, R. K. Gupta, W.Greiner, J. Phys. G: Nucl. Part. Phys. **38** 105101 (2011).

[12] M. K. Sharma, S. Kanwar, G. Sawhney, R. K. Gupta, and W. Greiner, J. Phys. G **38**, 055104 (2011); D. Jain, R. Kumar, M. K. Sharma, and R. K. Gupta, Phys. Rev. C **85**, 024615 (2012).

[13] K. Sandhu, M. K. Sharma, R. K. Gupta, Phys. Rev. C **85**, 014609 (2012).

[14] M. Kaur, R. Kumar, M. K. Sharma, Phys. Rev. C **85**, 014609 (2012); M. Kaur and M. K. Sharma Phys. Rev. C **85**, 054605 (2012).

[15] R. K. Gupta, M. Balasubramaniam, R. Kumar, D. Singh, C. Beck and W. Greiner, Phys. Rev. C **71**, 014601 (2005).

[16] J. Maruhn and W. Greiner, Z. Phys. **251,** 431 (1972).

[17] J. Maruhn and W. Greiner, Phys. Rev. Lett. **32**, 548 (1974).

[18] R. K Gupta, W. Scheid, and W. Greiner, Phys. Rev. Lett. **35**, 353 (1975).

[19**]** R. K. Gupta and W. Greiner, Heavy Elements and Related New Phenomena, World Scientific, Singapore, edited by W. Greiner and R.K Gupta, Vol.**I**, 397, (1999).

[20] S. S Malik and R. K. Gupta, Phys. Rev. C **39,** 1992 (1989).

[21] R. K. Gupta, W. Scheid and W. Grenier, J. Phys. G; Nucl. Part. Phys.**17** (1991); S. Kumar and R. K. Gupta, Phys. Rev. C **49,** 1922 (1994).

[22] S. Kumar and R. K. Gupta, Phys. Rev. C **55,** 218 (1997); R. K. Gupta, S. K. Arun, R. Kumar and Niyti Int. Rev. Phys. (IREPHY) **2**, 369 (2008).

[23] N. J. Davidson, S.S. Hsiao, J. Markram, H.G. Miller, and Y. Tsang, Nucl. Phys. A **570**, 61C (1994).

[24] P. A. Seeger, Nucl. Phys. **81**, 1 (1966).

[25] W. Myers and W. J. Swiatecki, Nucl. Phys. A **81**, 1 (1966).

[26] C. Y. Wong, Phys. Rev. Lett**. 31**, 1179 (1985).

[27] R. Aroumougame and R. K. Gupta, J. Phys. G **6**, L155 (1980).

[28] J. Blocki, J. Randrup, W. J. Swiatecki and C.F. Tsang, Ann . Phys. (NY) **105**, 427 (1977)

[29] Deryagin, Kolloid Z. **69**,155 (1934).

CHAPTER-3

3.1 Results and Discussion:-

In the present work, the dynamical cluster decay model DCM [1-5] based upon the quantum mechanical fragmentation theory (QMFT) [6-7] is applied here to understand the decay of superheavy nuclei ranging Z=102-113 [8-17]. The excitation function of various superheavy nuclei are calculated in the energy range E^*_{CN}=10.61-28.9 MeV, using β_2-deformations with hot optimum orientations. Earlier DCM has been applied for a variety of nuclei such as $^{297}117^*$[4], $^{291}115^*$[4], $^{290,292}114^*$ [5], $^{278,286}112^*$ [18] to understand the dynamics of superheavy mass region. In the decay of these nuclei via 2*n*-5*n* neutron evaporation, various factors such as fragmentation potential, preformation probability and penetration probability are analysed through which a detailed analysis of reaction dynamics can be estimated. In the present work DCM[8-17] based on the collective clusterization approach is used to investigate the *1n* evaporation channel of Z=102-113 superheavy nuclei. In the process, following points are investigated:-

(1) The role of hot and cold optimum orientations are studied for the decay of different superheavy nuclei.

(2) Effect of deformations on the decay path of superheavy nuclei is analyzed through fragmentation approach.

(3) Finally the importance of sticking moment of inertia (I_S) is advocated for 1n-decay of various superheavy nuclei.

First, to opt the favourable orientation approach for the decay of superheavy nuclei, the comparison of hot and cold optimum orientations are made in the DCM framework. The optimum orientations in DCM are given for cold, non-compact and hot, compact configurations corresponding to the largest interaction radius/lower barrier and the smallest interaction radius/highest barrier respectively [19]. With the cold orientation approach the calculated *1n* channel cross-sections are underestimated by significant amount, hence do not fit to the available experimental data. However, the use of hot optimum orientations with β_2-deformations seem to work nicely for the 1*n*-decay channels of majority of superheavy nuclei ranging Z=102-113. Within this approach, the channel cross-sections of superheavy nuclei are fitted nicely for Z=102-109 superheavy nuclei. Hence hot optimum configuration is considered as reasonably better approach for understanding the 1*n* decay of superheavy nuclei formed in cold fusion reactions.

It is relevant to mention here that DCM is based on well-known Quantum mechanical fragmentation theory which is exploited extensively to address cold fusion process during last about four decade. Within this cold fusion approach, one may employ hot as well as cold orientation configurations respectively in reference to compact and non-compact target projectile combinations.

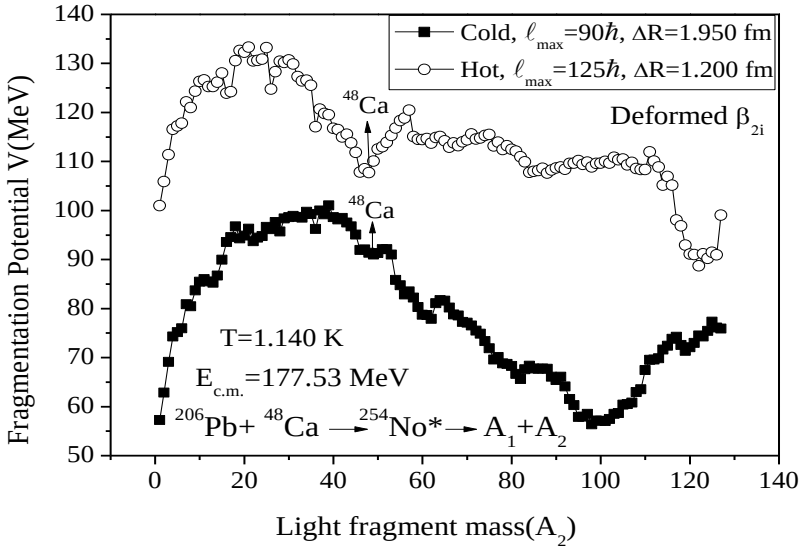

Fig.3.1 Fragmentation potential plot for the decay of ^{254}No as a function of fragment mass for both Hot and Cold orientations.*

To explore this point further, the fragmentation potential is plotted as the function of fragment mass (A_2) as shown in Fig.3.1 for hot as well as cold orientation approaches for the reaction ^{208}Pb + ^{48}Ca ^{254}No*. One can clearly see that there is a cold valley across ^{48}Ca (projectile) in case of hot configuration whereas the same is considerably suppressed for cold orientation approach. Hence in the further calculations we attempt to use exclusively the hot orientation approach to address *1n* decay mechanism of superheavy nuclei formed via a variety of heavy ion reactions.

Next, to explore the effect of deformations in the decay of SHN, we have compared the spherical and deformed choices of fragmentation for ^{254}No* and ^{267}Mt*, at the same neck-length parameter (ΔR) taken for the deformed case. It is relevant to mention here that the comparison of the fragmentation potential is shown here for Z=102 and Z=109 nuclei because the channel cross-sections are fitted only for $Z_{CN} \leq 109$ superheavy nuclei with β_2 deformations and optimum orientations. Hence to understand the structural changes governed through deformed fragmentation approach, we have chosen two extreme superheavy cases.

From Fig.3.2, one can observe that the spherical fragmentation potential show smooth variation with fragment mass whereas relatively more structure can be observed for the deformed choice of fragmentation. The structure in the fragmentation of the deformed case gives an idea about the probable decaying fragments which lie at the *minima* of the potential energy surfaces. The corresponding decay of $^{254}No^{*}$ and $^{267}Mt^{*}$ compound nuclei show minima in the PES for the heavy mass fragments (HMF's) as well as for the fission region (indicated in Fig.3.2). On the other hand, no indication of such *minima* can be observed for the spherical fragmentation approach. In addition to this, the lower fragmentation for evaporation residue channel also favours the neutron evaporation from $^{254}No^{*}$ and $^{267}Mt^{*}$compound nuclei. It is relevant to mention here that such structure in fragmentation potential V (MeV) is seen for the decay of all superheavy nuclei (Z=102-109) taken into consideration for spherical as well as deformed fragmentation approaches.

In order to compare the fragmentation potential of two different superheavy nuclei i.e. $^{254}No^{*}$ and $^{267}Mt^{*}$, it has been observed that the HMF and fission region are slightly modified while going from lighter to heavier compound nucleus. However, other regions like evaporation residues (ER) and intermediate mass fragments (IMF) show identical decay pattern for both nuclei with spherical and deformed fragmentation approaches.

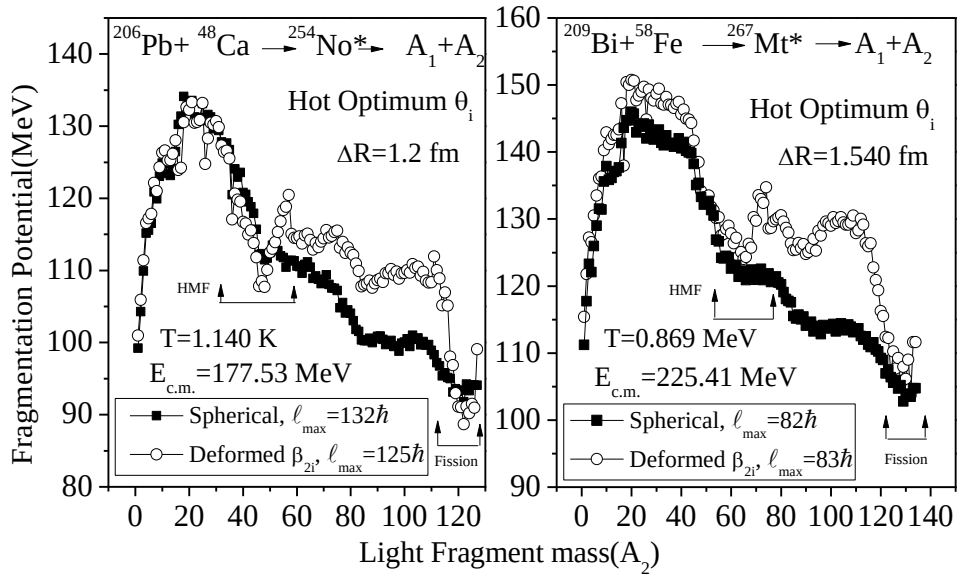

Fig.3.2. Fragmentation potential for the decay of $^{254}No^{*}$ and $^{267}Mt^{*}$ as a function of fragment mass at $\ell=\ell_{max.}$ for deformed as well as for spherical approach.

Further to observe the change in the fragmentation path for different even and odd-Z_{CN} superheavy nuclei we have plotted Fig.3.3 at different excitation energies of the compound nucleus. In Fig.3.3 (a), the variation of fragmentation potential with fragment mass is shown for even nuclei whereas Fig.3.3.(b) is plotted for odd superheavy nuclei. It is observed that the fragmentation path for neutron evaporation channels ($A_2 \leq 4$) and intermediate mass fragments ($5<Z<20$) remains identical for even-Z_{CN} SHN. However, the change in the heavy mass fragments (HMF) lying in mass range 40-90 and fission fragments can be seen in Fig. 3.3.(a). Also, on increasing the mass and the charge of the superheavy nuclear systems, the region of deep minima for HMF get shifted towards the higher mass of decaying fragments. It is relevant to mention here that the different magnitude of the fragmentation potential is due to the different excitation energies (equivalently temperature) chosen for even-Z nuclei but here we are interested in analysing the significant structural changes in the fragmentation paths for different mass regions.

From Fig. 3.3 (b), it is clear that almost similar results can be depicted for odd-Z_{CN} superheavy nuclei. Here also the major changes in the fragmentation path are observed for HMF and fission region. However the range of HMF region is slightly modified to 50-90 as compared to even-Z_{CN} superheavy nuclei.

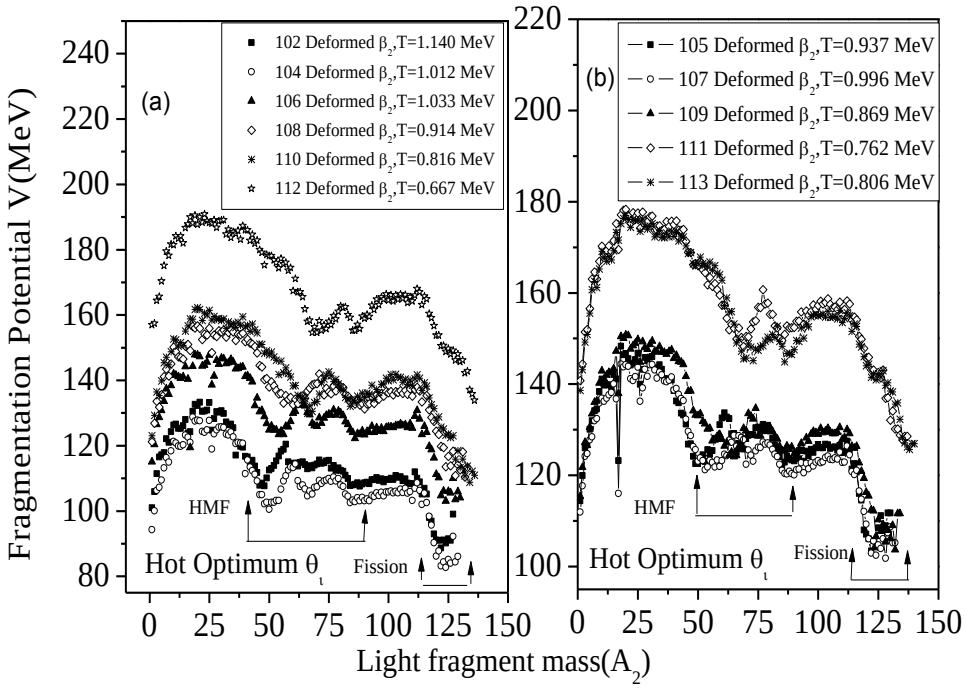

Fig.3.3 Fragmentation potential paths plotted for even and odd superheavy nuclei ranging Z_{CN}=102-113 as a function of fragment mass (A_2).

Next, the preformation probability (P_0) which is an important parameter of dynamical cluster decay model (DCM) is calculated for various superheavy nuclei. P_0 is the probability with which the cluster or fragment is preformed before it comes out of the compound system by penetrating the potential barrier. It is a relative quantity, i.e., a slight change in the potential for any one of the fragments leads to redistribution of P_0 among all the fragments. Fig 3.4 describes the variation of P_0 with fragment mass (A_i) for ^{254}No* and ^{267}Mt* nuclei at maximum value of angular momentum i.e. $\ell=\ell_{max}$. The careful observation of Fig.3.4 (a) and (b) reveals that the symmetric mass distribution of fission fragments is seen in two extreme cases depicted in Fig.3.4 for the decay of lighter as well as higher superheavy nuclei.

However, significant change in the distribution of preformation probability (P_0) for the heavy mass fragments is observed for ^{254}No* and ^{267}Mt* superheavy nuclei. The change in the HMF region consistent with the observation of Fig.3.3. But as the magnitude of this HMF peak is negligibly small, so it is not expected to continue toward total cross-sections of chosen reactions.

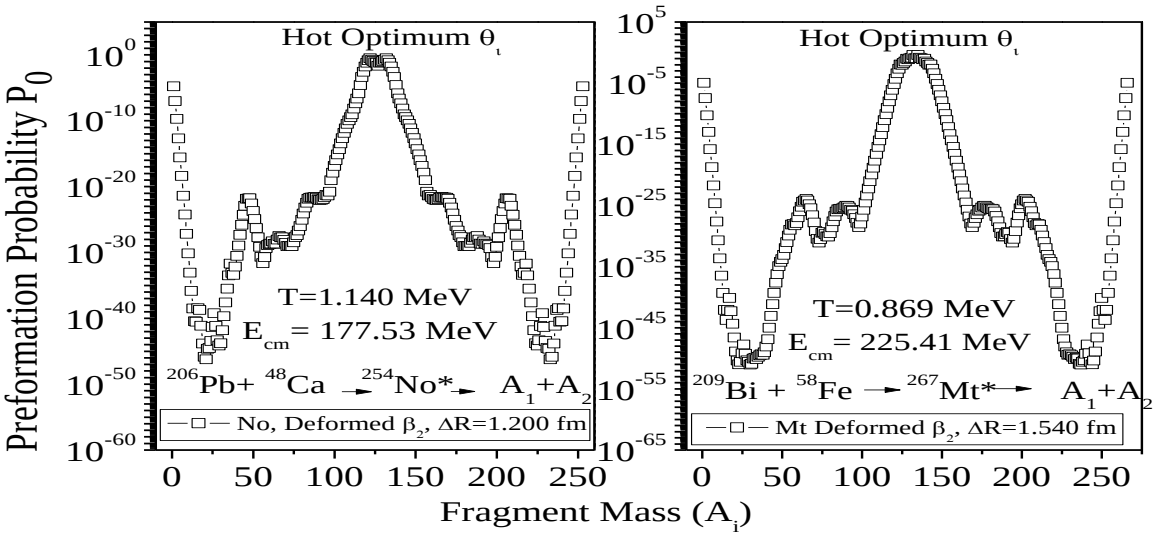

Fig.3.4 Preformation probability as a function of fragment mass (A_i) for the decay of ^{254}No and ^{267}Mt* superheavy nuclei.*

Another factor which contributes towards cross-section is the penetration probability P. Fig 3.5 shows the penetration probability (P) for ^{254}No* and ^{267}Mt* superheavy nuclei. The penetration probability P remains almost constant for the maximum range of the fragment masses in the decay of ^{267}Mt* compound nucleus. Broadly speaking, for HMF's, almost no

variation is obtained for the decay of Z_{CN}=109 nucleus, whereas structural fluctuation in the HMF region (90-160) can be seen in the penetration path of ^{254}No*.

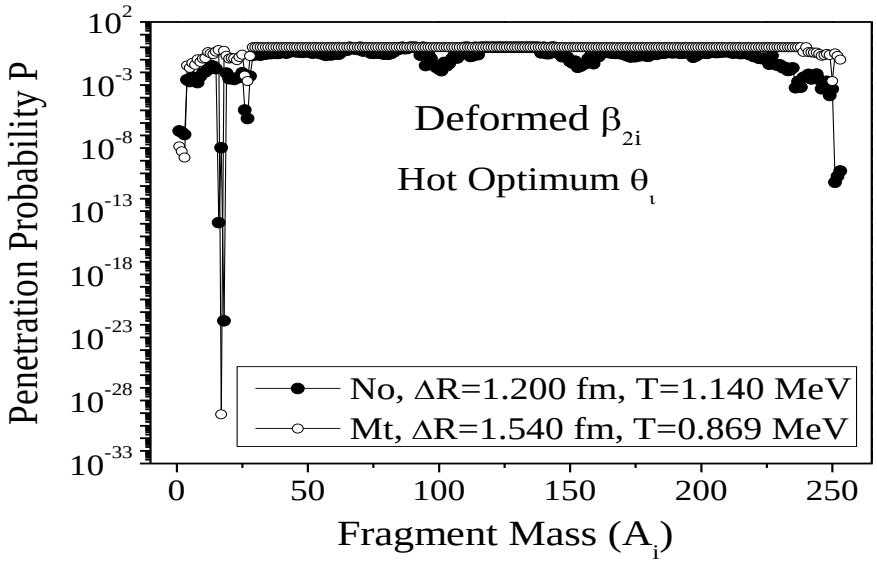

Fig.3.5. Penetration probability as a function of fragment mass for the decay of $^{254}No^{*}$ and $^{267}Mt^{*}$ superheavy nuclei.

Hence from above discussion it is clear that the penetration path changes slightly while going from lighter to heavier superheavy nuclei, particularly for the heavy mass fragments (HMF's), whereas almost identical penetration path is observed for the evaporation and fission region for all superheavy nuclei lying in the range Z_{CN}=102-109.

Using the preformation and penetration probability for the 1*n* decaying fragments, we have calculated the neutron channel cross-sections for Z_{CN}=102-113 superheavy nuclei. In DCM, the total cross section is calculated by summing the cross sections over all ℓ-values lying in the ℓ=0 to ℓ_{max} range [Eq. (2.3)], which otherwise give significant contribution only in the limited range of angular momentum window spread between ℓ_{min} to ℓ_{max}. Fig. 3.6 presents the variation of channel cross-section as a function of angular momentum to fix the ℓ-window for superheavy nuclei lying in range Z_{CN}=102-109. For example, the ℓ-window for 1*n* decay of $^{254}No^{*}$ is lying in the range ℓ=72-125 (ħ), whereas the ℓ -states spread in the range. ℓ=51-84(ħ) for the $^{267}Mt^{*}$ with intermediate nucleus ^{259}Db imparting ℓ-values in between the two. Further, the ℓ_{max} values decided from Fig.3.6, decrease with increase in the charge and mass of the superheavy nuclei, also as shown in table 1 and Fig. 3.6(b).

Fig.3.7, shows the variation of the maximum value of the angular momentum with the atomic number of the superheavy compound nuclei at their respective excitation energies. It is relevant to mention here that, in present analysis maximum value of excitation energy is chosen from [8-17] in reference to *1n* decay of the superheavy nuclei. From figure it is observed that the variation of ℓ_{max} is also in accordance with the excitation energy of the compound nucleus, more the excitation energy, higher is the angular momentum states. It simply mean that the excitation energy and angular momentum are crucial parameters to address the dynamics of heavy/superheavy nuclei.

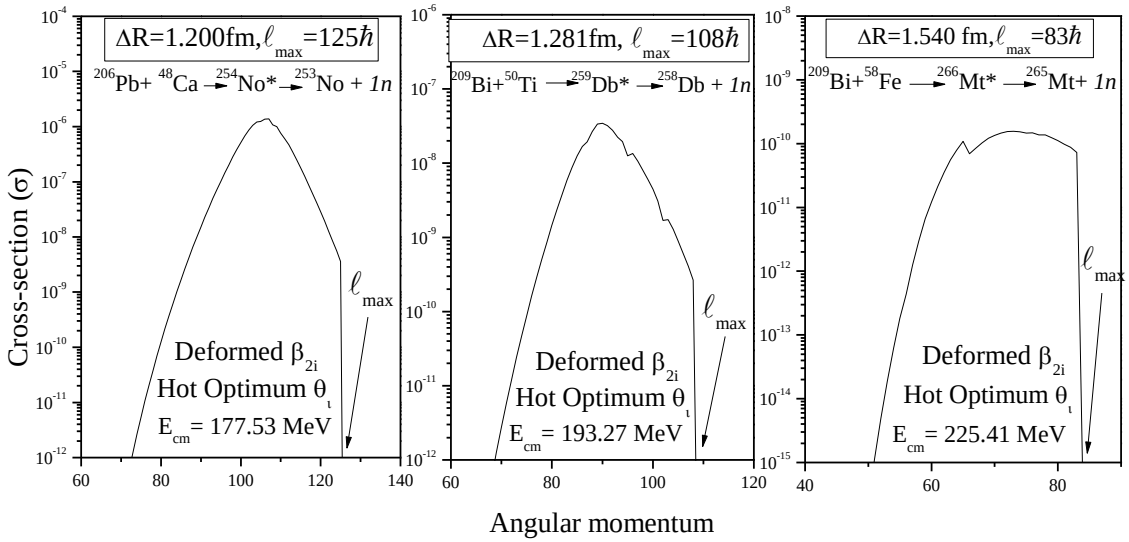

Fig.3.6.Variation of channel cross-section as a function of angular momentum for the decay of No, Db* and Mt* superheavy nuclei.*

Within the range of ℓ-windows, we have calculated the 1*n* channel cross-sections for Z_{CN}=102-113 superheavy nuclei. DCM calculated cross-sections show nice agreement with the experimental data [8-17] with deformed fragmentation approach for majority of the superheavy nuclei as shown in Fig. 3.8 and table 1. However heavier nuclei (Z_{CN}>109) could not be addressed nicely with the inclusion of the β_2- deformations. Hence it is relevant to mention that for representing the Fig.3.8 (a), the calculations are carried out for the use of sticking moment of inertia, explained in chapter 2. On the other hand, the non-sticking approach for the decaying fragments is also applied in the present work to address *1n* evaporation cross-sections of Z_{CN}=102-113 superheavy nuclei. For non-sticking approach, nice fitting of experimental data is obtained for all the superheavy nuclei except ^{278}112* nucleus,

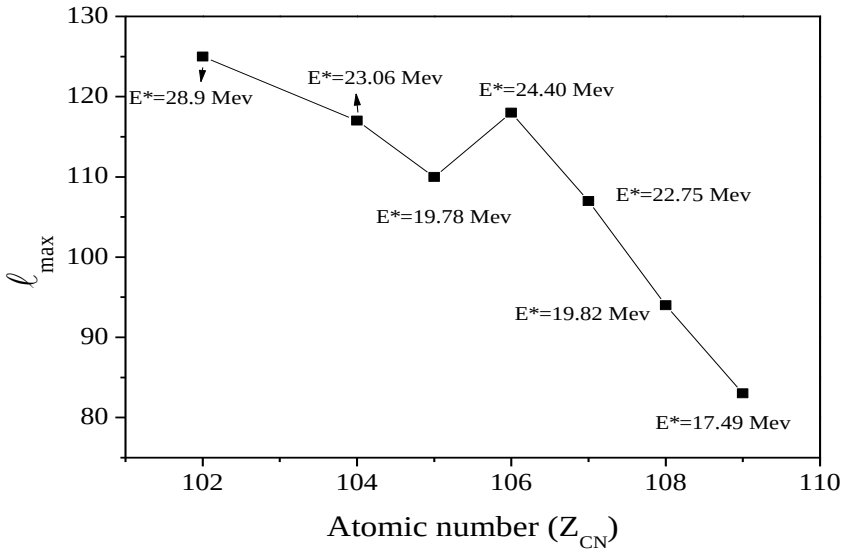

Fig.3.7. Variation of maximum value of angular momentum as a function of atomic number of superheavy nuclei ranging Z_{CN} =102-109.

Also one can visualize from Fig. 3.8 that the channel cross-sections decreases with increase in atomic number (Z_{CN}) of the compound nuclei. This is probably due to the fact that with increase in the mass of projectile the mass asymmetry in the entrance channel decreases which lead to small production cross-sections for superheavy elements.

Table 1, represents the comparison of experimental data studied in GSI, RIKEN, and LBNL [8-17] with DCM fitted cross-sections. The neck-length parameter ΔR, maximum value of angular momentum ℓ_{max} is also given below:

Z_{CN}	A_{CN}	E* (MeV)	$E_{c.m}$ (MeV)	T (MeV)	ℓ_{max} (ħ)	$\Delta R(I_S)$ (fm)	σ_{DCM} (I_S)	$\Delta R(I_{NS})$ (fm)	σ_{DCM} (I_{NS})	σ_{Exp}
102	254	28.90	177.53	1.140	125	1.200	14.7 nb	0.538	15.8 nb	≤15 nb
104	258	23.06	193.46	1.012	115	1.235	0.822 nb	0.983	0.826 nb	0.803 nb
105	259	19.78	193.27	0.937	108	1.281	0.334 nb	1.041	0.375 nb	0.384 nb

106	262	24.40	211.75	1.033	117	1.182	0.0871 nb	0.975	0.0812 nb	0.0867 nb
107	263	22.75	213.48	0.996	107	1.240	0.033 nb	1.039	0.036 nb	0.0341 nb
108	266	19.82	224.99	0.914	94	1.370	0.00231 nb	1.052	0.00207 nb	0.00223 nb
109	267	17.49	225.41	0.869	83	1.540	2.50 pb	1.072	2.74 pb	2.57 pb
110	272	15.69	240.28	0.816	63	1.950	0.275 pb	1.080	16.0 pb	15.43 pb
111	273	13.66	241.88	0.762	62	1.700	2.23×10^{-6} pb	1.128	2.62 pb	2.77 pb
112	278	10.61	255.75	0.667	65	1.850	8.37×10^{-20} pb	1.300	0.0403 pb	0.511 pb
113	279	15.68	261.46	0.806	57	1.800	1.66×10^{-5} pb	1.082	0.0338 pb	0.0305 pb

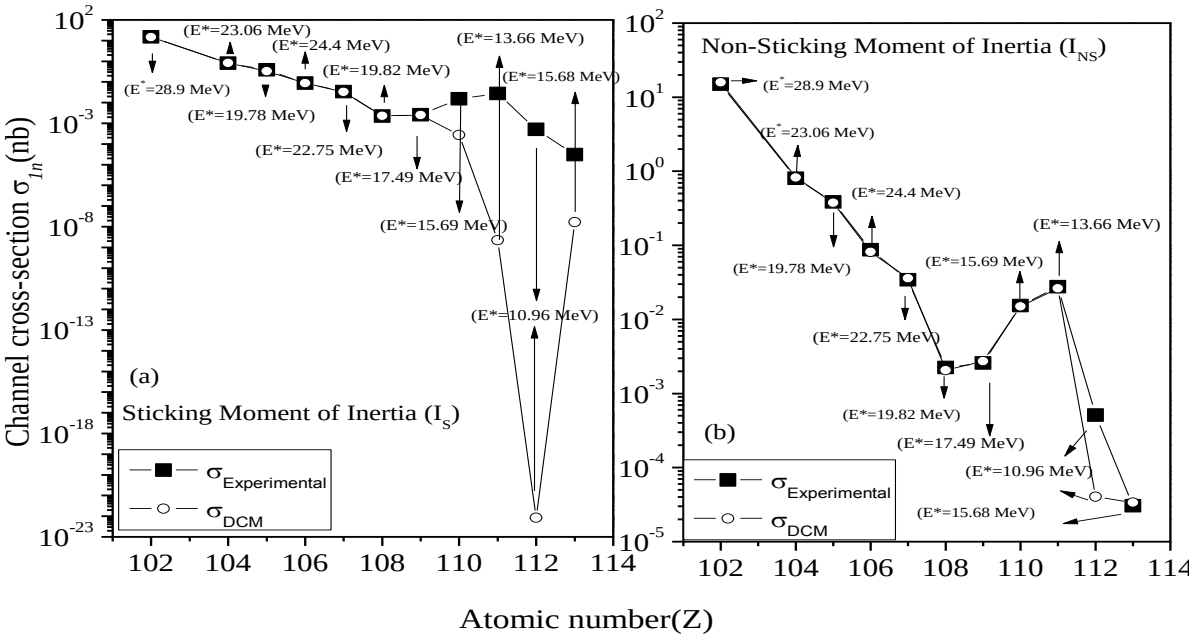

Fig.3.8. DCM calculated 1n cross-sections plotted as a function of atomic number varying from Z_{CN}=102-113, in the energy range 10.61-28.9 MeV for (a) sticking moment of inertia (b) non-sticking moment of inertia and compared with the experimental data of [8-17].

The variation of neck-length parameter (ΔR) with atomic number of the compound nucleus is shown in Fig.3.9. for 1*n* decay channel of deformed choice of fragments. Fig3.9 (a) show the variation for the case when the decaying fragments follows sticking approach of moment of inertia, whereas the neck-length parameter (ΔR) is mentioned in the Fig.3.9 (b) for non-sticking moment of inertia. It is clear from figure that as we increase Z_{CN}, the neck length parameter (ΔR) also shows increasing behaviour for both formalisms. The comparative analysis of Fig3.9. (a) and Fig.3.9. (b) shows that for non-sticking approach, the lower magnitude of neck-length parameter is involved as compares to I_S.

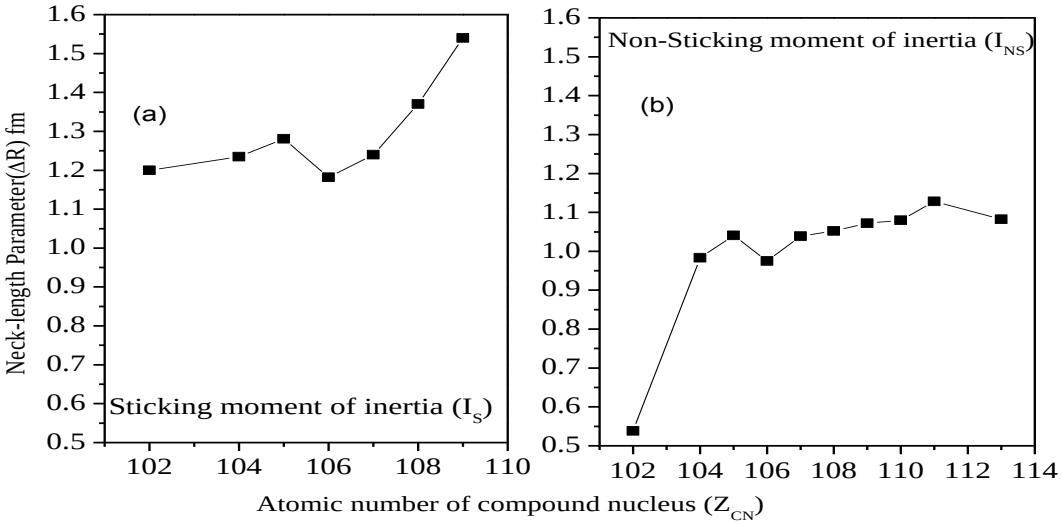

Fig.3.9. Variation of neck-length parameter (ΔR) for (a) sticking moment of inertia (b) non-sticking moment of inertia with atomic number of superheavy nuclei ranging Z_{CN} =102-109.

Finally to understand the role of sticking (I_S) and non-sticking moment of inertia (I_{NS}) for 1*n* decay of superheavy nuclei, we have plotted the Fig 3.10 and 3.11 respectively for even-Z_{CN} and odd- Z_{CN} nuclear systems. The Gaussian variation of the channel cross-section with angular momentum as shown in Fig.3.6, is the prime requirement in the partial wave formalism, and equivalently in DCM. Interestingly, it is observed only for the sticking approach of moment of inertia (I_S). On the other hand the non-sticking (I_{NS}) approach, used to address the channel cross-section do not impart Gaussian character for superheavy nuclei as shown in the Fig 3.10 and Fig.3.11. Figure 3.10 is plotted for the even Z_{CN} superheavy nuclei whereas odd superheavy nuclei are shown in Fig.3.11. Hence one can clearly say that sticking moment of inertia (I_S) still a preferred choice despite of the fact that non-sticking approach

fits the data for higher superheavy nuclei with Z>109 and exhibit relatively smaller neck-length values.

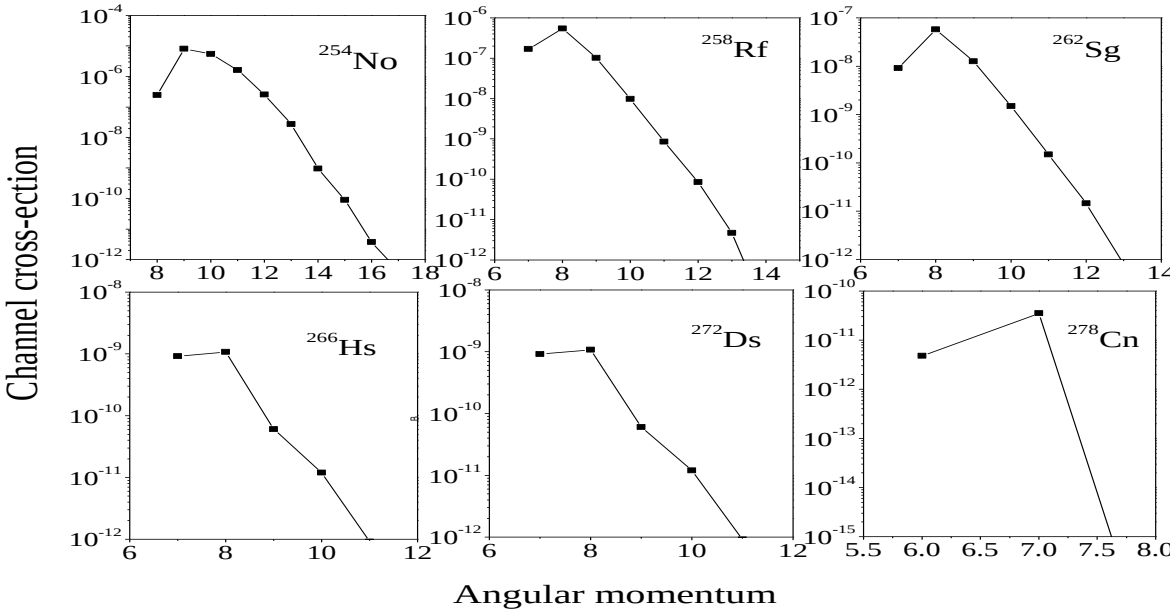

Fig.3.10 Variation of channel cross section with angular momentum for non-sticking moment of inertia (I_{NS}) for even superheavy nuclei.

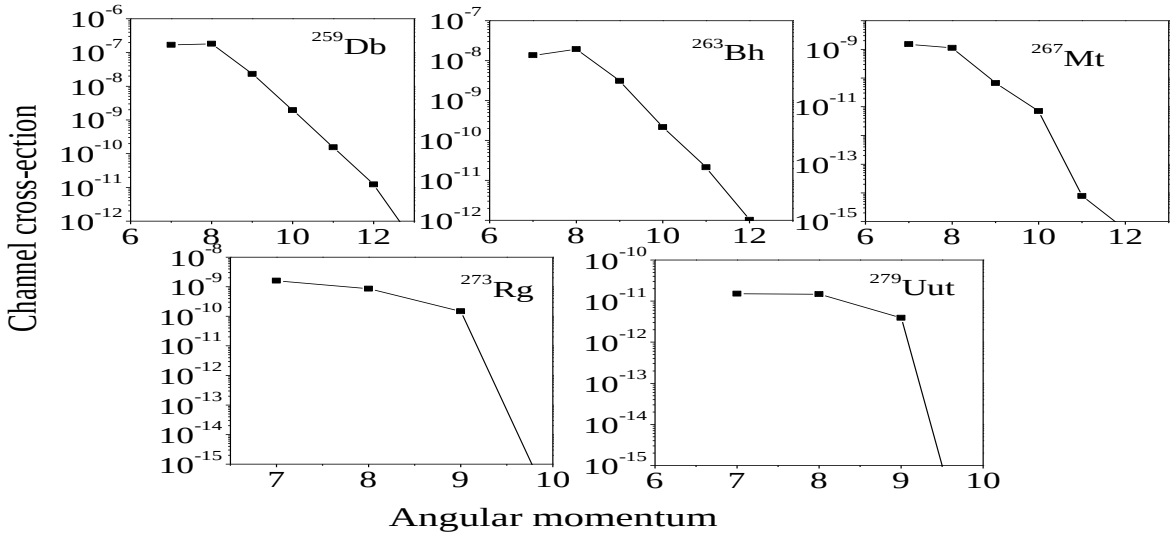

Fig.3.11 Variation of channel cross section with angular momentum for non-sticking moment of inertia (I_{NS}) for odd superheavy nuclei.

3.2 Summary:-

In the present work, the 1*n*-decay of Z_{CN}=102-113 superheavy nuclei is studied in the wide energy range of E*=10.61-28.9 MeV via dynamical cluster decay model (DCM). The decay of compound nuclei formed in the cold fusion is studied via hot optimum configuration as the cold configurations of the decaying fragments do not fit the experimental data nicely. More structure in the fragmentation path is seen for deformed fragmentation approach as compared to the spherical one. With inclusion of deformations upto β_2 within hot optimum approach, the channel cross-sections are fitted nicely within the experimental limits for the superheavy nuclei $Z_{CN}\leq 109$. A comparative analysis of sticking and non-sticking moment of inertia is also made to account for exclusive role of rotational energy term in the dynamics of chosen relations. Although data of higher charge/mass superheavy nuclei with Z>109 could be fitted with non-sticking approach but the use of sticking moment of inertia is advocated as the earlier don't impact expected Gaussian behaviour when *1n* evaporation cross-sections are plotted as a function of angular momentum. It would be of further interest to investigate the *1n* evaporation channel of chosen nuclei by employing different nuclear interactions exhibiting a variety of barrier profiles so as to reach at the final conclusion regarding dynamical evaluation of these superheavy systems.

References:

[1] R.K. Gupta, M. Balasubraniam, C.Mazzocchi, M. La Commara and W. Scheid, Phys. Rev. C 64, 024601 (2002).

[2] B. B. Singh, M. K. Sharma, R. K. Gupta and W.Greiner, Int. J. Mod. Phys. E15, 699 (2006) ; B. B. Singh, M. K. Sharma, R. K. Gupta, Phys. Rev. C 77, 054613 (2008).

[3] M. K. Sharma, S. Kanwar, G. Sawhney, R. K. Gupta, and W. Greiner, J. Phys. G **38**, 055104 (2011); D. Jain, R. Kumar, M. K. Sharma, and R. K. Gupta, Phys. Rev. C **85**, 024615 (2012).

[4] K. Sandhu, M. K. Sharma and R. K. Gupta, Phys. Rev. C **85**, 024604 (2012), R. Kumar, K. Sandhu, M. K. Sharma and R. K. Gupta, Phys. Rev. C **87**, 054610 (2013).

[5] K. Sandhu, M. K. Sharma, Braz. J. Phys **44**, 64 (2014), K. Sandhu, G. Kaur, M. K. Sharma, Nucl. Phys.A, **921**, 114 (2014).

[6] J. Maruhn and W. Greiner, Z. Phys. **251,** 431 (1972).

[7] J. Maruhn and W. Greiner, Phys. Rev. Lett. **32**, 548 (1974).

[8] Yu. Ts. Oganessian, V. K. Utyonkov, Yu. V. Lobanov, F. Sh. Abdullin, A. N. Polyakov, I. V. Shirokovsky, Yu. S. Tsyganov, A. N. Mezentsev, S. Iliev, V. G. Subbotin, A. M. Sukhov, K. Subotic, O. V. Ivanov, A. N. Voinov, and V. I. Zagrebaev , Phys. Rev. C **64,** 054606 (2001).

[9] I. Dragojevic, K. E. Gregorich, Ch. E. Dullmann, M. A. Garcia, J. M. Gates, S. L. Nelson, L. Stavsetra, R. Sudowe and H. Nitsche, Phys. Rev. C **78**, 024605 (2008).

[10] J. M. Gates, S. L. Nelson, K. E. Gregorich, I. Dragojevic, Ch. E. Dullmann, P. A. Ellison, C. M. Folden, M. A. Garcia, L. Stavsetra, R. Sudowe, D. C. Hoffman, and H. Nitsche, Phys. Rev. C **78**, 034604 (2008).

[11] S. Hofmann, Rep. Prog. Phys. **61**, 639 (1998),

[12] S. L. Nelson, C. M. Folden, K. E. Gregorich, I. Dragojevic, Ch. E. Dullmann, R. Eichler, M. A. Garcia, J. M. Gates, R. Sudowe and H. Nitsche, Phys. Rev. C **78**, 024606 (2008).

[13] S. Hofmann, F.P. Heberger, V. Ninov, P. Armbruster, G. M ¨unzenber, C. Stode, A.G. Popeko, A.V. Yeremin, S. Saro, M. Leino, Z. Phys. A **358**, 377–378 (1997).

[14] K. Morita, K. Morimoto, D. Kajib, S. Gotoc, Eur. Phys. J. A **21**, 257 (2004); K. Morita K. Morimoto, D. Kajib, S. Gotoc, Nucl. Phys. A **734**, 101 (2004).

[15] K. Morita, K. Morimoto, D. Kajib, S. Gotoc., J. Phys. Soc. Jpn. **76**, 043201 (2007).

[16] K. Morita, K. Morimoto, D. Kajib, S. Gotoc.,J. Phys. Soc. Jpn. **73**, 2593 (2004).

[17] T. Cap and K. Siwek-Wilczynska, Phys. Rev. C **83,** 054602 (2011).

[18] K. Sandhu, G. Kaur, M. K. Sharma, Nucl. Phys.A, **921**, 114 (2014).

[19] R.K. Gupta, M. Balasubraniam, R. Kumar, N. Singh, J.Phys.G, Nucl.Part.Phys **31**, 631-644 (2005).